

Nonlinear Photophysics and Ablation of Liquid Naphthalene Derivatives: Fluence-Dependence of Luminescence Spectra upon 248 nm Laser Excitation

Yasuyuki Tsuboi,* Kentaro Irie, Hiroshi Miyasaka,† and Akira Itaya

Department of Polymer Science and Engineering, Kyoto Institute of Technology, Matsugasaki, Sakyo-ku, Kyoto 606-8585, Japan

Received: July 15, 2002; In Final Form: December 31, 2002

The ablation of liquid naphthalene derivatives (1-methylnaphthalene and 1-chloronaphthalene) induced by 248-nm pulsed excimer laser irradiation was investigated by means of a photoacoustic technique and by nanosecond time-resolved luminescence/absorption spectroscopy. Cavitation (ablation) was observed in both of the liquids when the laser fluence was increased beyond a certain threshold. During the photoacoustic measurements, the ablation threshold was evaluated to be 20 mJ/cm² for both of the liquids. In the time-resolved luminescence spectroscopy, two spectral components were detected both above and below the threshold: the fluorescence of naphthalene monomers and the fluorescence of excimers. The former component is conspicuous in the later temporal stage after the excitation. One characteristic feature observed in the luminescence spectroscopy below the threshold region was that the ratio of the intensity of the monomer fluorescence to the excimer fluorescence increased with increasing laser fluence. This behavior, that is, the increase in the monomer component, was also induced by raising the temperature of the liquids. No chemical intermediates such as radicals (which would suggest photochemical fragmentation) were detected by the transient absorption spectroscopy during ablation. These results indicate that a photothermal effect is dominant for laser ablation in liquid naphthalene derivatives. The temperature at the ablation threshold was estimated on the basis of the intensity ratio of the monomer and excimer fluorescence components and the Boltzmann equilibrium.

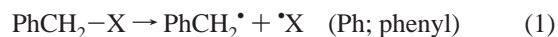
1. Introduction

Interactions between laser light sources and absorbing liquids are of great interest in terms of nonlinear photophysics and photochemistry. Under excitation at sufficiently low intensities, normal relaxation processes such as fluorescence, internal conversion, intersystem crossing, excimer formation of solvent or solute molecules, and so forth are observed. With increasing excitation intensity, various nonlinear processes are induced. A macroscopic morphological change such as bubble formation (cavitation) accompanied by the emission of sound and visible light is one of these processes, which takes place when a certain threshold is reached in the excitation intensity. In 1988, R. Srinivasan et al. found such a phenomenon (cavitation and shock-sound generation) for liquid (neat) benzene irradiated with a pulsed KrF excimer laser.¹ They named this macroscopic morphological change liquid ablation and ascribed the fundamental process of the ablation to a photochemical decomposition mechanism.

According to many preceding investigations, the dominant processes responsible for ablation fall into two categories: photochemical and photothermal mechanisms.² In the former case, concentrated direct scission of chemical bonds takes place following UV photon absorption, and consequent volume explosion leads to ablation. In the latter case, temperature

elevation due to the efficient conversion of energy from light to heat by internal conversion and vibrational relaxation leads to a thermal mechanism. Of course, both of these mechanisms are interrelated with each other and cannot be completely separated in real processes, and especially in 248 nm ablation. In the case of polymeric solids, which have attracted much attention in the research field of the ablation of organic materials, the structures are microscopically inhomogeneous with respect to conformation, cross-linking, tacticity, and so on, and these complexities prevent a comprehensive elucidation of the mechanism of ablation. By contrast, molecular liquids represent an ideal system for investigating the ablation mechanisms, since the liquids are deemed to be homogeneous and isotropic structures.

One of the authors (Y.T.) has investigated the 248-nm laser ablation of liquid benzene and related derivatives by means of a photoacoustic technique and by nanosecond time-resolved spectroscopic/imaging measurements.^{3–7} From these investigations, it was deduced that the ablation thresholds are not correlated with the boiling points of the liquids but with their photochemical reactivity.



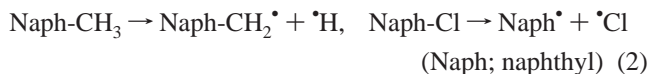
The ablation threshold decreased with increasing quantum yield for the photochemical fragmentation. During fragmentation, a transient species (the benzyl radical (PhCH₂·)), could be clearly detected by time-resolved absorption spectroscopy. On the basis of these results, the fundamental mechanism of benzene ablation was concluded to be a photochemical process; that is, the photochemical reaction generates 0.05 M benzyl radical and

* Corresponding author. Present address: Division of Chemistry, Graduate School of Science, Hokkaido University, Sapporo 060-0810, Japan. Also at PRESTO (Precursory Research for Embryonic Science and Technology), "Structure and Transformation", JST (Japan Science and Technology Corporation). E-mail: twoboys@sci.hokudai.ac.jp.

† Present address: Department of Chemistry, Faculty of Engineering Science, Osaka University, Toyonaka, Osaka 560-8531, Japan.

the corresponding gaseous molecules (X_2), which results in a volume explosion (ablation). This photochemical ablation mechanism was supported by recent theoretical modeling by Zhigilei and Garrison.^{8,9} They confirmed that photochemical fragmentation assists the efficiency of the ablation process in the benzene system by carrying out molecular dynamics simulations. On the other hand, we also highlighted the photothermal mechanism in the ablation of organic solutions of aromatics (phenanthrene/ethanol, etc.),¹⁰ since the ablation threshold increased as the boiling point of the solvent increased. The temperature at the ablation threshold reached the boiling point of the sample solvent. Such a relationship between the ablation threshold and the boiling point was never observed in the ablation of liquid benzenes. In addition, hot bands were clearly detected in the fluorescence spectra of solute molecules upon ablation; that is, the ablation of the solutions is brought about by explosive boiling. Thus, the apparent mechanism of liquid ablation varies from system to system. The ablation of a liquid polymer has also been investigated recently, when it was found that aspects of ablation in the liquid state differ from those in the solid state.¹¹

In the present study, we focused our attention on the photo-physical processes and ablation behavior of liquid naphthalene derivatives from the viewpoint of laser-fluence dependence. Several researchers have investigated the photochemistry and photophysics of naphthalene derivatives in solution and in the gas phase.¹² However, reports on the photochemistry and photophysics of neat liquid naphthalene derivatives have been very limited so far.^{13,14} To obtain further insight into the mechanistic aspects of liquid ablation, we investigated the pulsed laser ablation of neat 1-methylnaphthalene and 1-chloronaphthalene by means of a photoacoustic technique and by nanosecond laser photolysis measurements. Both of these substances are in the liquid phase at room temperature. In addition, these naphthalene molecules have several similar features to those of the benzene derivatives: both of them have large conjugated π -electronic systems, both form excimers, and both have photochemical reactivities.



Therefore, it is intriguing to compare the ablation behavior between liquid naphthalenes and benzenes. The photoacoustic technique is quite an effective way of evaluating the ablation thresholds of liquids, while the spectroscopic measurements give us a wealth of information on the photophysical and photochemical dynamics of liquids. On the basis of the experimental results, we discuss the ablation mechanism in terms of photochemical and photothermal processes.

2. Experimental Section

1-Methylnaphthalene (Tokyo Kasei, EP grade) and 1-chloronaphthalene (Wako, GR grade) were purified by alumina column chromatography and distillation under reduced pressure. The purity of the liquids was checked from the absorption tail in the longer-wavelength region and from the fluorescence: no emission arising from impurities was detected for both of the liquids. The liquids were deoxygenated by bubbling with N_2 .

A KrF excimer laser (Lambda Physik, EMG-201, 248 nm, fwhm \sim 20 ns) was used as an excitation light source. The laser fluence was adjusted by using attenuators and was measured with a power meter (Gentec, ED-200). A PZT ceramic (Murata Co. Ltd.) attached to a quartz cell (optical length = 1 cm) was used as a piezoelectric transducer to detect the

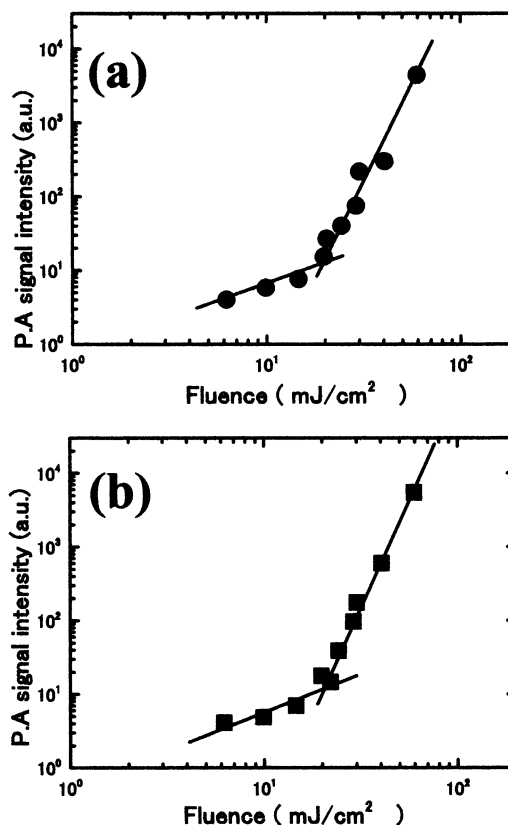


Figure 1. Logarithmic plots of photoacoustic (PA) signal intensity as a function of laser fluence for the liquids (a) 1-MN (1-methylnaphthalene) and (b) 1-CN (1-chloronaphthalene). In both parts of the figure, breaking points can be clearly recognized at 20 mJ/cm². This value is regarded as being the ablation threshold.

photoacoustic signals. The photoacoustic signals were amplified with a homemade amplifier and detected with a digital oscilloscope (LeCroy, 9314C). The maximum of the first significant peak was taken in the usual manner.^{4,5} Nanosecond time-resolved luminescence and absorption spectra were measured with a computer-controlled nanosecond laser photolysis system. The optical alignments were similar to those described in a previous paper.¹⁵ Briefly, a gated multichannel photodiode array (Hamamatsu, PMA-50 system) with a polychromator (Acton, M4197) was used as a detector. A pulsed Xe lamp was used as a probe light source. The excimer laser and the detector system were electrically synchronized by a delay and pulse generator (Stanford research, DG535), and the timing was monitored with an oscilloscope. The temporal profile of luminescence was measured with a monochromator equipped with a photomultiplier tube. A ceramic heater was attached to the sample cell, and the temperature was controlled using a controller (Omron, E5EX) with a thermocouple. The steady-state absorption and fluorescence spectra were measured with Shimadzu MPS-2000 and Hitachi F-4500 spectrometers, respectively.

3. Results and Discussion

Photoacoustic Measurement. Figure 1 shows the photoacoustic (PA) signals plotted against the laser fluence for neat 1-methylnaphthalene (1-MN) and 1-chloronaphthalene (1-CN). Both axes are on logarithmic scales. In both cases, it is possible to find apparent breaking points around a fluence value of 20 mJ/cm². Below the breaking points, the PA signal increases with an increase in the fluence, and the slope is almost unity, indicating that normal one-photon processes are responsible for

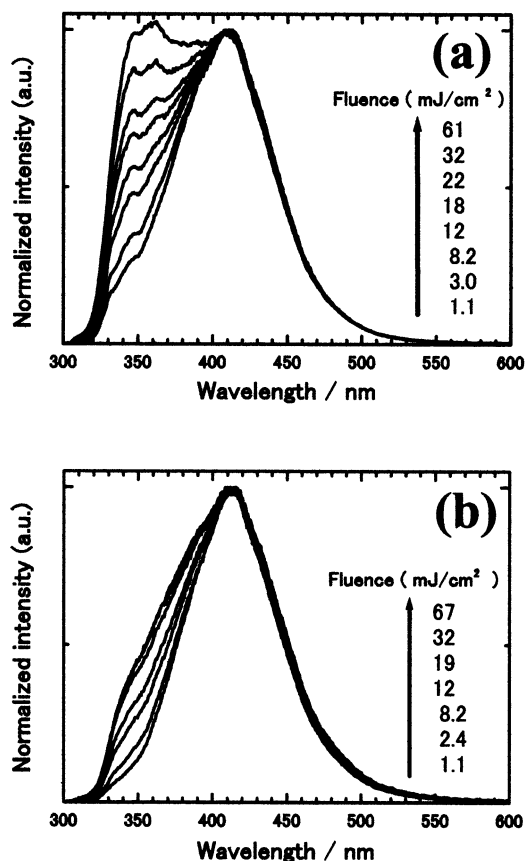


Figure 2. Time-integrated luminescence spectra for (a) 1-MN and (b) 1-CN excited at the various laser fluences given in the figures. All the spectra are normalized at 410 nm. The broad bands with peak positions at this wavelength are ascribable to the naphthalene excimers, while the bands located around the shorter wavelength (~ 350 nm), which become appreciable with increasing laser fluence, are assigned to naphthalene monomers.

the PA signal.¹⁶ In this fluence region of ≤ 20 mJ/cm², the absorbed light energy increases with increasing laser fluence, and consequently the PA signal increases due to radiationless transitions such as internal conversion and excimer formation. Above the breaking point, the PA signal increases abruptly, showing a nonlinear dependence. In this fluence region (> 20 mJ/cm²), the formation of bubbles (cavitation) was recognized in the liquids by visual observation.

In previous studies of the UV laser ablation of liquid benzene derivatives,^{4–6} the ablation (cavitation) thresholds were determined by means of photoacoustic and nanosecond imaging techniques.^{4–7} The fluences at the breaking point agreed well with the thresholds determined by the nanosecond imaging for each benzene derivative. In the same way, the fluence at the breaking point (20 mJ/cm²) was adopted as the ablation threshold for 1-MN and 1-CN. When ablation takes place, the mechanical stresses due to the formation of the bubbles and their collapse in the liquids contribute to the PA signal, resulting in an abrupt jump in the signal, as shown in Figure 1.

Time-Integrated Luminescence Spectroscopy. Time-integrated luminescence spectroscopy was carried out below and above the ablation threshold. In Figure 2, the time-integrated luminescence spectra of liquid 1-MN (a) and 1-CN (b) are shown at various fluences. The luminescence spectra of both of the liquids are normalized at 410 nm. The broad spectra with a peak position at 410 nm can safely be assigned to the excimers of 1-MN and 1-CN in accordance with the figures given in the literature.^{12,17} The spectra taken at the lowest fluence (1.1 mJ/

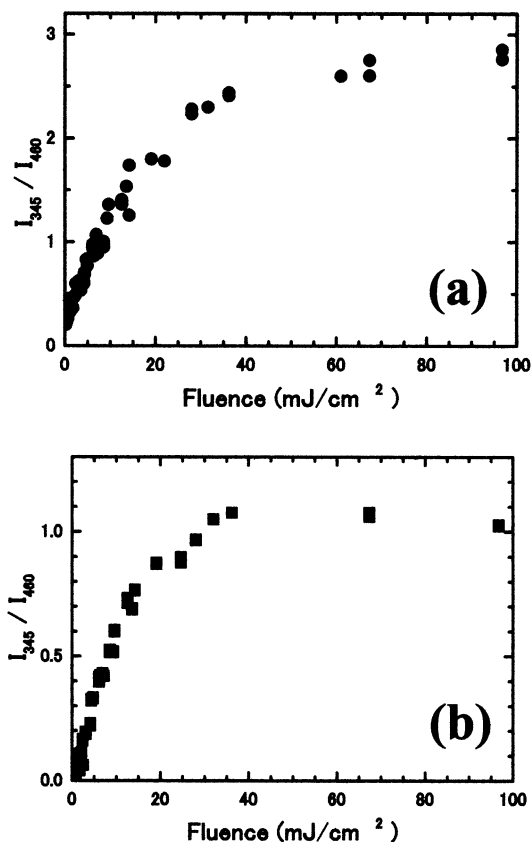


Figure 3. Ratios of the time-integrated luminescence intensity of the monomer (I_{345}) to that of the excimer (I_{460}) for (a) 1-MN (a) and (b) 1-CN. The intensities of the monomer and the excimer are taken at 345 and 360 nm, respectively, in Figure 2. The saturation of the ratios is observable above the ablation threshold of 20 mJ/cm².

cm²) agreed with those obtained by steady-state measurements. For both of the liquids, a dependence of the spectral shape with respect to the fluence was clearly observed. For 1-MN (a), the fluorescence with vibrational structures around 340 nm becomes appreciable as the fluence increases. This emission band is ascribable to the 1-MN monomer fluorescence, in accordance with the literature.¹⁷ Other than the excimer and monomer fluorescence, no emission was observed for other species such as radicals over the wavelength windows examined here, even when the fluence was higher than the threshold. Also, for 1-CN (b), an enhancement of the monomer fluorescence with increasing fluence is observable, although the degree of enhancement is lower than the case of 1-MN.

In Figure 3, the ratios of the fluorescence intensities (I_{345}/I_{460}) are plotted against the laser fluence for both of the liquids, where I_{345} and I_{460} are the intensity of the monomer fluorescence measured at 345 nm and that of the excimer measured at 460 nm, respectively. At this wavelength of 460 nm, the contribution from the monomer fluorescence is negligible. In the figure, a nonlinear relationship between the ratio and the fluence can be clearly seen for both of the liquids. In the lower fluence region (< 20 mJ/cm²), the ratios increase, while, in the higher fluence region (> 20 mJ/cm²), the values of the ratios tend to saturate. It is worth noting that the fluence value at this turning point was almost the same as the ablation threshold (20 mJ/cm²) as determined by the photoacoustic measurements. This coincidence implies that the origin of this saturation behavior has a strong correlation with the laser ablation.

Photothermal Effect. Here we consider the origin of the fluence dependence of the fluorescence spectra. An enhancement

of the monomer fluorescence under high fluence irradiation was also observed for solid polystyrene irradiated with a 248 nm excimer laser.¹⁸ It has been established that laser ablation of polystyrene is brought about photothermally.^{18–20} Such an enhancement of the monomer fluorescence can be interpreted within a thermal picture. The radiationless process should elevate the temperature in the irradiated domain. Accordingly, the dynamic equilibrium between the monomer and the excimer states shifts toward the higher (monomer) state. By analogy to the case of polystyrene, we deduce that the origin of the fluence-dependent fluorescence spectra is also a photothermal effect in the present case.

To examine this deduction, the temperature dependence of the time-integrated luminescence spectra was measured by excitation with a very low fluence (0.3 mJ/cm²). Figure 4 shows the temperature dependence of the time-integrated luminescence spectra normalized at 410 nm for 1-MN and 1-CN. The monomer fluorescence increases with increasing temperature, similar to the observation in Figure 3. The results strongly suggest that the enhancement of the monomer fluorescence with increasing laser fluence can mainly be interpreted in terms of a photothermal effect that was induced by radiationless transitions following the laser excitation.

The intensity ratio of the monomer and the excimer emissions is a function of the temperature. Here we assume that the degree of thermal quenching of the fluorescence does not differ between the monomer and excimer. Then, from the temperature dependence of the ratios and the Boltzmann distribution, we can evaluate the energy gap between the excited monomer state and the excimer state (ΔE) from the following equation

$$\ln \frac{I_{345}}{I_{460}} = -\frac{\Delta E}{kT} + \text{constant} \quad (3)$$

where I_{345} and I_{460} are the fluorescence intensities of the monomer taken at 345 nm and the excimer taken at 460 nm, respectively. T and k are the temperature of the liquid and the Boltzmann constant, respectively. Figure 5 exhibits the relationship between $\ln(I_{345}/I_{460})$ and the reciprocal of the temperature. A linear relationship was observed for both of the liquids. The ΔE values for 1-MN and 1-CN could be obtained from the slopes of the linear relationship, and these were determined to be 2.2×10^3 and 2.1×10^3 cm⁻¹, respectively. These values of ΔE are in good agreement with the values reported elsewhere for naphthalene derivatives (2×10^3 cm⁻¹).^{13,14,21} Using the temperature-sensitive spectral shape and the ratio of (I_{345}/I_{460}), we can estimate the temperature of the liquid naphthalenes.

By using this thermal picture, we can interpret the fluence-dependent ratio of ($I_{\text{monomer}}/I_{\text{excimer}}$) shown in Figure 3, since the fluence and temperature dependences of the spectral shape are qualitatively similar to each other. As previously pointed out, normal photothermal processes are dominant when the fluence is below 20 mJ/cm². The excited molecules rapidly release vibrational energy to the surrounding liquid molecules through a radiationless transition, resulting in a temperature elevation.²² Accordingly, the saturation of the ratios above the ablation threshold suggests that part of the excitation energy was not used for increasing the temperature of liquids but for inducing the morphological change, that is, laser ablation. In other words, part of the excitation energy is consumed for the ablation.

Nanosecond Time-Resolved Spectroscopy. To elucidate the time scale of the temperature elevation and the ablation mechanism, nanosecond time-resolved spectroscopy was em-

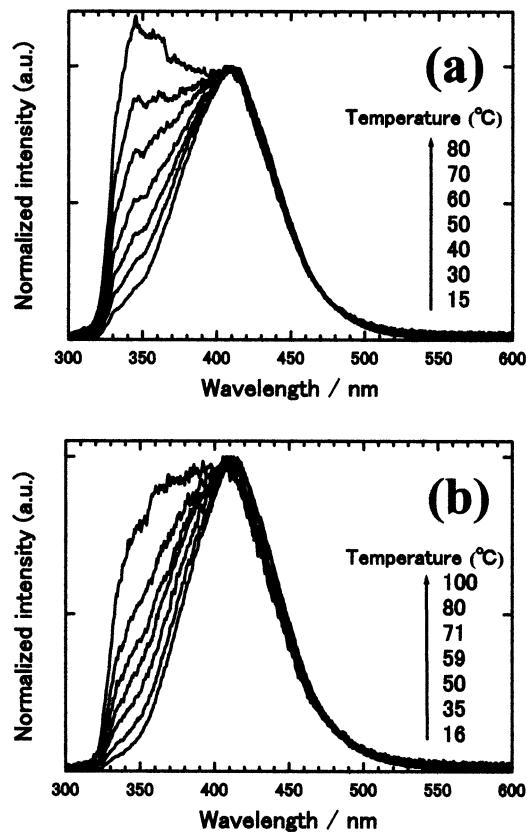


Figure 4. Temperature dependence of the time-integrated luminescence spectra obtained at a very low fluence of 0.3 mJ/cm². The temperature is given in the figures for (a) 1-MN (a) and (b) 1-CN. A spectral evolution similar to the case of the fluence effect (Figure 2) is also seen in this case.

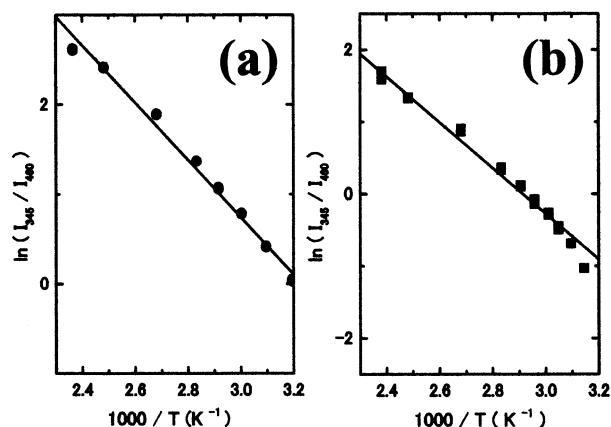


Figure 5. Semilogarithmic plots of the ratios of the luminescence intensity of the monomer to that of the excimer against the inverse of the temperature. In both parts of the figure, (a) 1-MN and (b) 1-CN, the plots show a linear relationship.

ployed. Figure 6 displays the fluence dependence of the time-resolved emission spectra of 1-MN (a) and 1-CN (b) excited with a nanosecond 248-nm laser pulse. The temporal origin ($t = 0$) is defined as the time when the onset of the rise of the laser pulse (fwhm ~ 20 ns) was detected. Gate-timings for the detection were 5–10 and 30–35 ns, corresponding to the former and later parts of the pulse, respectively. Namely, all the transient spectra described below were temporally obtained within the pulse duration.

In the time-resolved fluorescence spectra during the early stage (5–10 ns, dotted line in Figure 6), only the broad excimer bands around 410 nm are observed for both of the liquids over

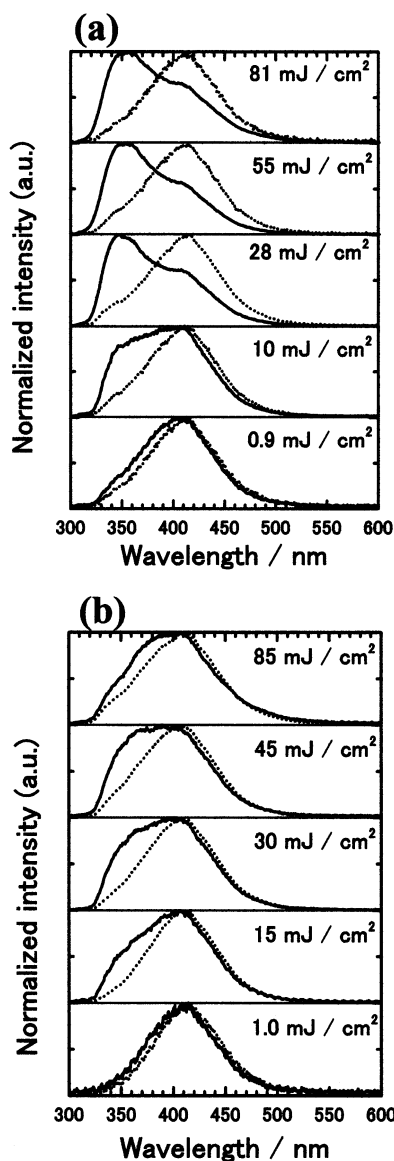


Figure 6. Time-resolved luminescence spectra for (a) 1-MN and (b) 1-CN at the various fluences given in the figure. The gate time for the detection is 5–10 ns (dotted line) and 30–35 ns (solid line). Only the excimer emissions are observed in the early stages, while the monomer emissions are conspicuous during the later stages.

a wide range of fluence. For neat liquid aromatics (benzene and naphthalene derivatives), exciton migrations followed by structural rearrangements lead to excimer formation with a sandwich-type configuration.^{14,23–25} This process takes place on the order of a few picoseconds, that is, approximately, a few tens of picoseconds. Therefore, the spectra in the early stage can be ascribed to the equilibrium state between the monomer and the excimer. On the other hand, the emission spectra in the later stages (30–35 ns, solid line in Figure 6) apparently exhibit fluence dependencies; that is, one can find an increase in the monomer fluorescence with an increase in the fluence. Since the equilibrium between the monomer and the excimer is attained within the observed temporal regime, the spectral behavior of the fluence dependence may be understood in terms of the photothermal effect. In accordance with the increase in the fluence, the temperature at the irradiated domain rises, resulting in a shift of the equilibrium toward the excited monomer state. The temporal evolution of the spectra reflects the dynamics of temperature elevation. The temperature elevation should be already achieved within the excited pulse, whose

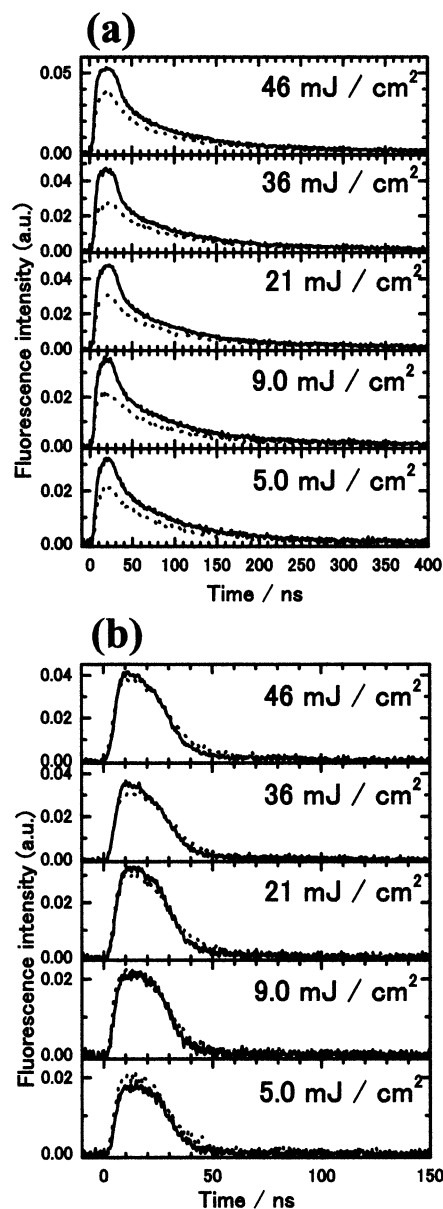


Figure 7. Temporal profile of the fluorescence for (a) 1-MN (a) and (b) 1-CN. The monomer fluorescence (solid line) and the excimer fluorescence (dotted line) are measured at 345 and 460 nm, respectively. Laser fluence is given in the figure.

temporal duration is 40 ns, due to a rapid radiationless transition such as internal conversion followed by vibrational cooling.

In Figure 7, temporal profiles of the monomer and the excimer fluorescence are shown for 1-MN (a) and 1-CN (b). In both parts of the figure, the monomer fluorescence (monitored at 345 nm, solid line) and the excimer fluorescence (monitored at 460 nm, dotted line) exhibit the same temporal behavior. This is consistent with the fact that the monomer and the excimer are in an equilibrium state in the temporal window observed here. For 1-MN, the lifetimes of the monomer (in toluene) and the excimer (in neat liquid) states are 70 and 60 ns, respectively.^{12a} These values are very close to each other and much larger than the time constant for the formation and dissociation of the excimer state. Therefore, both of these states roughly follow a quasi-single-exponential decay with a time constant close to these values. Indeed, the tail parts ($t > 50$ ns) of the temporal profile of 1-MN irradiated at 5.0 mJ/cm² (bottom panel of part a) were analyzed with a single-exponential function to give a time constant of ~ 70 ns. This component hardly depends on

the laser fluence, as shown in the figure. However, the rise and decay dynamics at the early stage (0–30 ns) seems to be slightly affected by the laser fluence. With increasing fluence, these concentrated excited states should be generated to induce interactions between the excited states: S_1-S_1 annihilation. Such a process is involved under these intense irradiation conditions and is reflected in the time profile of the fluorescence. For 1-CN, the lifetime of the monomer state is 2.4 ns (in hexane).^{12a} This value is much smaller than the duration time of the excitation pulse (~40 ns), and hence the temporal profiles of the monomer and the excimer states should trace that of the excitation pulse. Also, in 1-CN, the rise and decay dynamics in the early stages (0–30 ns) are slightly affected by laser fluence. The annihilation process is involved under intense irradiation. Such an annihilation process would partly contribute to the temperature elevation.

In the photochemical laser ablation of liquid benzene derivatives, monomer fluorescence with a small contribution from the excimer fluorescence was detected around the ablation thresholds.²⁶ However, we did not detect any such fluence and temporal dependencies of the emission spectra observed for the present liquid naphthalene derivatives (Figures 2, 3, and 6).^{4,5} On the other hand, the transient species (benzyl radical) produced by the photochemical decomposition was clearly detected in the ablation process of the liquid benzenes.⁵ For 1-MN and 1-CN, we measured nanosecond time-resolved absorption spectra over a wide range of wavelength (350–800 nm). However, no significant absorption signal was detected for both of the liquids. According to the literature, various transient species of naphthalene derivatives such as the excited singlet and triplet states of monomers ($S_n \leftarrow S_1$ and $T_n \leftarrow T_1$ absorption),²⁷ anionic and cationic radicals,²⁸ and 1-naphthylmethyl radical²⁹ have absorption bands in this wavelength region. Among them, $S_n \leftarrow S_1$ and $T_n \leftarrow T_1$ absorptions of naphthalene derivatives have very low values of molar extinction coefficients, and hence the excited species would hardly be detected. Ionic species, which are generated by multiphotonic excitations, should not be generated with long lifetimes due to the low polarity of the liquid naphthalenes. The 1-naphthylmethyl radical has a sharp absorption around 380 nm. In addition, the fluorescence spectrum of the 1-naphthylmethyl radical is located around 600 nm.³⁰ As already described, no emission was detected around 600 nm for liquid 1-methylnaphthalene. These results imply that the contribution from the photochemical decomposition is quite minor in the present case and is consistent with the discussions of the photoacoustic measurement and the time-integrated luminescence spectroscopy. A large part of the absorbed energy would be consumed to elevate the temperature of the liquids.

Ablation Mechanism in Liquid Naphthalene Derivatives.

The above experimental results on the transient species and the fluence-dependent behavior lead to the conclusion that the photochemical effects that are observed in liquid benzene ablation are negligible for the present case. On the other hand, spectral behavior depending upon the laser fluence and the temperature strongly suggests an efficient photothermal process in the present ablation. In organic solutions of aromatics (phenanthrene/ethanol, etc.), laser ablation is induced by explosive boiling due to the photothermal effect.¹⁰ In this case, the solutions are heated above their boiling points upon ablation due to the efficient conversion from light energy to heat by the solute aromatics.

For a quantitative discussion, we will attempt to estimate the temperature at the ablation threshold using numerical calculation and our experimental results. The temperature at the threshold,

T_{th} , is estimated using the following well-known equation,³¹ on the assumption that the Lambert–Beer's law holds and the absorbed light energy is completely converted into heat

$$T_{th} = T_{room} + \Delta T \quad (4)$$

$$\Delta T = \alpha F_{th} / \rho C \quad (5)$$

where α , ρ , and C are the absorption coefficient, the density, and the specific heat of the liquids, respectively. T_{room} and F_{th} are room temperature and the ablation threshold, respectively. The use of eqs 4 and 5 seems valid, since the photothermal effect is obvious for the liquids. T_{th} is evaluated to be 600 and 560 K for 1-MN and 1-CN. These T_{th} values are slightly higher than the boiling points of the corresponding liquids (517.8 K for 1-MN and 535.7 K for 1-CN).³² On the other hand, it was revealed that the ratio (I_{345}/I_{460}) is very sensitive to the temperature of the liquids. Hence, we can also estimate T_{th} by using the ratio of the fluorescence intensity (I_{345}/I_{460}) at 30–35 ns in the transient spectra and the relationship in Figure 5. The estimated T_{th} is 390 K for 1-MN and 400 K for 1-CN. These values are somewhat lower than those estimated numerically and do not reach the boiling points.

The reason the values of T_{th} contradict each other (numerical and experimental) is somewhat complicated and ambiguous at present. The main error in using eqs 4 and 5 is the decrease of the temperature rise (ΔT) due to the nonthermal deactivation: fluorescence. For naphthalene derivatives, the quantum efficiency of the monomer and the excimer fluorescence is ~0.3,²¹ and accordingly ΔT should be decreased by a factor of 0.7. Then, taking this into account, T_{th} should be corrected to be ~500 K. At present, we consider that the real values of T_{th} lie in the range 400–500 K. The value is close to the boiling points, but not close enough to induce ablation by explosive boiling. Other effects may also be involved in the present ablation. One candidate for a tentative explanation would be a contribution from a photoacoustic wave.³³ Such an effect has been reported to assist the pulsed laser ablation of an aqueous solution of $CuCl_2$. In the present case, the absorption coefficient (α) is very high ($3 \times 10^4 \text{ cm}^{-1}$)³⁴ compared to that of neat benzene ($2 \times 10^3 \text{ cm}^{-1}$).^{1,5} Therefore, a local acoustic stress wave with an intense amplitude would be generated in the irradiated domain. This mechanical stress probably contributes to the present ablation of liquid naphthalene derivatives.

Concerning the photochemistry of naphthalene, Georgiou et al. investigated the photochemical behavior of iodonaphthalene-doped polymer (PMMA) films under 248 and 193 nm ablation by means of a laser-induced fluorescence (LIF) technique.^{35, 36} When the doping concentration was increased, they observed a new broad fluorescence band and assigned it to a (naphthalene)₂-type species. However, no such species was observed in the present spectroscopic measurements. In their experiments the laser fluence was 10 times as large as that in the present case. Therefore, the (naphthalene)₂-type species may be formed by multiphotonic decomposition of iodonaphthalene. In addition, rapid excimer formation would prevail in the decomposition in 1-CN. Furthermore, 1-CN has a relatively low yield for decomposition (2) in the condensed phase, since the monomer fluorescence is clearly observable. If LIF measurements were to be applied to the present system, such a photoproduct may be slightly detected. Also, such a photochemical decomposition possibly contributes in a small way to the present ablation.

4. Concluding Remarks

For liquid naphthalene derivatives, photophysical behavior induced by 248-nm laser excitation was investigated by a

photoacoustic technique and spectroscopic methods in terms of the fluence dependence. Ablation (cavitation) was observed beyond a threshold value of 20 mJ/cm². Time-integrated and time-resolved spectroscopy revealed that photothermal effects due to radiationless transitions following the excitation have an important role in the photophysical behavior. No radical or chemical intermediates indicative of a photochemical process were detected by the time-resolved absorption spectroscopy. Hence, the photochemical effect observed in liquid benzene derivatives should be negligible for the present systems. For laser ablation, the temperature at the ablated domains was evaluated by both numerical and experimental methods. This value ranges from 400 to 500 K, which is close to or somewhat lower than the boiling points of the liquids. Contributions from an acoustic wave may be involved in the present ablation.

We concluded that the photothermal effect has a remarkable influence with increasing fluence in the liquid naphthalene systems that we studied. On the other hand, it has been reported that, for the laser ablation of liquid benzene derivatives, the photochemical process is dominant. These differences in behavior are of interest in terms of the photophysics and the photochemistry of liquid aromatic molecules.

Acknowledgment. We would like to thank Dr. T. Suzuki (Tokyo Institute of Technology) for useful information on the transient spectra of naphthalene derivatives. We are also grateful to Dr. T. Moriyama (Kyoto Institute of Technology) for his technical support with the photoacoustic apparatus. This work was partly supported by a Grant-in-Aid from the Ministry of Education, Culture, Sports, Science and Technology of Japan to Y.T. (No. 13750669).

References and Notes

- (1) Srinivasan, R.; Ghosh, A. P. *Chem. Phys. Lett.* **1988**, *143*, 546.
- (2) Srinivasan, R.; Braren, B. *Chem. Rev.* **1989**, *89*, 1303.
- (3) Tsuboi, Y.; Fukumura, H.; Masuhara, H. *Appl. Phys. Lett.* **1994**, *64*, 2745.
- (4) Tsuboi, Y.; Hatanaka, K.; Fukumura, H.; Masuhara, H. *J. Phys. Chem.* **1994**, *98*, 11237.
- (5) Tsuboi, Y.; Hatanaka, K.; Fukumura, H.; Masuhara, H. *J. Phys. Chem. A* **1998**, *102*, 1661.
- (6) Hatanaka, K.; Kawao, M.; Tsuboi, Y.; Fukumura, H.; Masuhara, H. *J. Appl. Phys.* **1997**, *82*, 5799.
- (7) Hatanaka, K.; Tsuboi, Y.; Fukumura, H.; Masuhara, H. *J. Phys. Chem. B* **2002**, *106*, 3049.
- (8) Zhigilei, L. V.; Garrison, B. J. *J. Appl. Phys.* **2000**, *88*, 1281.
- (9) Yingling, Y. G.; Zhigilei, J. V.; Garrison, B. J. *J. Photochem. Photobiol., A: Chem.* **2001**, *145*, 173.
- (10) Tsuboi, Y.; Fukumura, H.; Masuhara, H. *J. Phys. Chem.* **1995**, *99*, 10305.
- (11) Hopp, B.; Smausz, T.; Wittman, T.; Ignacz, F. *Appl. Phys. A* **2000**, *71*, 315.
- (12) (a) Mataga, N.; Tomura, N.; Nishimura, H. *Mol. Phys.* **1965**, *6*, 367. (b) Cai, J.; Lim, E. C. *J. Phys. Chem.* **1990**, *94*, 8357. (c) Cai, J.; Lim, E. C. *J. Phys. Chem.* **1992**, *96*, 8265. (d) Saigusa, H.; Sun, S.; Lim, E. C. *J. Phys. Chem.* **1992**, *96*, 10099.
- (13) Ohno, T.; Kato, S. *Chem. Lett.* **1976**, 263.
- (14) Ohno, T.; Kato, S. *Bull. Chem. Soc. Jpn.* **1981**, *54*, 1517.
- (15) Itaya, A.; Kitagawa, T.; Moriyama, T.; Matsushita, T.; Miyasaka, H. *J. Phys. Chem. B* **1997**, *101*, 524.
- (16) Cross, F. W.; Al-Dhahir, R. K.; Dyer, P. E. *J. Appl. Phys.* **1988**, *64*, 2194.
- (17) Berlman, I. B. *Handbook of Fluorescence Spectra of Aromatic Molecules*; Academic Press: New York, 1971.
- (18) Tsuboi, Y.; Sakashita, S.-I.; Hatanaka, K.; Fukumura, H.; Masuhara, H. *Laser Chem.* **1996**, *16*, 167.
- (19) Tsunekawa, M.; Nishio, S.; Sato, H. *J. Appl. Phys.* **1994**, *76*, 5598.
- (20) Feldmann, D.; Kutzner, J.; Laukemper, J.; MacRobert, S.; Weldge, K. H. *Appl. Phys. B* **1987**, *44*, 81.
- (21) Birks, J. B. *Photophysics of Aromatic Molecules*; Wiley-Interscience: London, 1970.
- (22) Miyasaka, H.; Hagihara, M.; Okada, T.; Mataga, N. *Chem. Phys. Lett.* **1992**, *259*, 188.
- (23) Hamanoue, K.; Hidaka, T.; Nakayama, T.; Teranishi, H. *Chem. Phys. Lett.* **1981**, *82*, 55.
- (24) Masuhara, H.; Miyasaka, H.; Ikeda, N.; Mataga, N. *Chem. Phys. Lett.* **1981**, *82*, 59.
- (25) Miyasaka, H.; Mataga, N. *J. Mol. Liq.* **1995**, *65/66*, 393.
- (26) Tsuboi, Y. Dr. Thesis, Osaka University, 1995.
- (27) Brun, A.; Harriman, A.; Tsuboi, Y.; Okada, T.; Mataga, N. *J. Chem. Soc., Faraday Trans.* **1995**, *91*, 4047.
- (28) Shida, T. *Electronic Absorption Spectra of Radical Ions*; Elsevier: Amsterdam, 1988.
- (29) Nagano, M.; Suzuki, T.; Ichimura, T. *J. Photochem. Photobiol., A: Chem.* **2001**, *140*, 15.
- (30) Kelley, D. F.; Milton, S. V.; Huppert, D.; Rentzepl, P. M. *J. Phys. Chem.* **1983**, *87*, 1842.
- (31) Fukumura, H.; Mibuka, N.; Eura, S.; Masuhara, H. *Appl. Phys. A* **1991**, *53*, 255.
- (32) *Kagaku Binran*, 3rd ed.; Maruzen: Tokyo, 1984 (in Japanese).
- (33) Golovlyov, V. V.; Letokhov, V. S. *Appl. Phys. B* **1993**, *57*, 417.
- (34) Measured in our laboratory.
- (35) Athanassiou, A.; Lassithiotaki, M.; Anglos, D.; Georgiou, S.; Fotakis, C. *Appl. Surf. Sci.* **2000**, *154/155*, 89.
- (36) Athanassiou, A.; Andreou, E.; Fragouli, D.; Anglos, D.; Georgiou, S.; Fotakis, C. *J. Photochem. Photobiol., A: Chem.* **2001**, *145*, 229.